Journal of Alloys and Compounds 509 (2011) 712–718

Contents lists available at ScienceDirect

Journal of Alloys and Compounds

journal homepage: www.elsevier.com/locate/jallcom

Characterization and electrochemical properties of carbon-coated $Li_4Ti_5O_{12}$ prepared by a citric acid sol–gel method

Jin Wang[a,b], Xiao-Min Liu[a], Hui Yang[a,*], Xiao-dong Shen[a]

[a] College of Materials Science and Engineering, Nanjing University of Technology, Nanjing 210009, PR China
[b] National Engineering Research Center for Nanotechnology, 28 East Jiangchuan Road, Shanghai 200241, PR China

ARTICLE INFO

Article history:
Received 3 March 2010
Received in revised form 29 July 2010
Accepted 30 July 2010
Available online 7 August 2010

Keywords:
Lithium-ion battery
Carbon coating
Spinel $Li_4Ti_5O_{12}$
Sol–gel

ABSTRACT

Since carbon coating can effectively improve electrical wiring of $Li_4Ti_5O_{12}$ and thus enhance its high rate performance, a novel and simple citric acid sol–gel method for in situ carbon coating is employed in this study. The effects of the amount of the carbon source in the starting xerogel on the particle size, the resistance and the electrochemical performance of the synthesized $Li_4Ti_5O_{12}$ samples are systematically studied. The physical and electrochemical properties of the obtained samples have been characterized by XRD, TG-DSC, SEM, TEM, BET, A.C. impedance, galvanostatically charge–discharge and cyclic voltammetry tests. The results show that the initial amount of the carbon source in the starting xerogel is a critical factor which determines the content of the coated carbon and the pore volume, therefore governs the high rate performance of the $Li_4Ti_5O_{12}$/C composites. The $Li_4Ti_5O_{12}$/C composite with in situ carbon coating of 3.5 wt% exhibits the best electrochemical performance which delivers delithiation capacities of 143.6 and 133.5 mAh g^{-1} with fairly stable cycling performance even after 50 cycles at 0.5C and 1C rate, respectively.

1. Introduction

Nowadays, safety issues have to be overcome in order to apply Li-ion batteries in some large-scale applications, such as electric vehicles and hybrid electric vehicles. Since solid electrolyte interface (SEI) film formed on the surface of graphite particles during first few cycles of lithium intercalation can initiate the thermal runaway of Li-ion batteries and cause safety problems [1–3], spinel $Li_4Ti_5O_{12}$ is a very promising anode material with high safety due to the absence of SEI film: its flat discharge platform at about 1.55 V versus Li^+/Li is above the reduction potential of most organic electrolytes (~0.8 V versus Li^+/Li) which can restrain the SEI film from the reduction of electrolytes and sufficiently avoid the formation of metallic lithium [4], therefore improving the safety of Li-ion batteries. In addition, $Li_4Ti_5O_{12}$ has some other advantages such as extremely small structural change during lithium insertion/extraction and high reversible capacity (175 mAh g^{-1}) [5,6]. However, its power performance is greatly limited by its low electronic conductivity [7]. Two typical approaches have been developed over the past few years to resolve this problem. One is to develop the nanoparticles, which can reduce the Li-ion diffusion path, as well as provide large contact area between the electrode and electrolyte [8–13]. The other is to improve the electrical conductivity by cation doping [5,7,14–18], surface modification with metals or their oxides [19–22], and carbon coating [13,14,23–26]. In these ways, carbon coating as one kind of surface treatment method has been managed in several kinds of electrode materials of Li-ion batteries due to its low cost and efficiency.

Solid-state method has been widely employed to synthesize $Li_4Ti_5O_{12}$/C composites [13,14,23–25]. Compared to the solid-state method, the sol–gel route is well known for its advantage in lowering heat temperature to obtain tailored particles [27]. Yang and Xu [28] reported an organic solvent based sol–gel method for the synthesis of in situ carbon-coated $LiMPO_4$ (M = Fe, Mn, Co, Ni) with excellent electrochemical performances. Such an organic solvent based sol–gel route offers a novel and simple method to synthesize carbon-coated $Li_4Ti_5O_{12}$ composites. In this paper, we report a citric acid sol–gel method to synthesize carbon-coated $Li_4Ti_5O_{12}$ composites. The relevant synthesis parameters and the physical characteristics of the synthesized $Li_4Ti_5O_{12}$/C composites are systematically investigated to obtain the target products with the best electrochemical performance.

2. Experimental

2.1. Synthesis of $Li_4Ti_5O_{12}$/C composites

$Li_4Ti_5O_{12}$/C composites were synthesized using $CH_3COOLi{\cdot}2H_2O$ (AR), tetrabutyl titanate [$Ti(OC_4H_9)_4$] (CP) and the citric acid (CP). Solution A and B were obtained by dissolving $CH_3COOLi{\cdot}2H_2O$ and $Ti(OC_4H_9)_4$ in ethanol, respectively. Solution A was

* Corresponding author. Tel.: +86 25 83587238; fax: +86 25 83587238.
E-mail address: yanghui@njut.edu.cn (H. Yang).

0925-8388/$ – see front matter © 2010 Elsevier B.V. All rights reserved.
doi:10.1016/j.jallcom.2010.07.215

added slowly to solution B with the mole ratio of Li to Ti equivalent to 1. The mixed solution was magnetically stirred at room temperature (RT) to get a transparent yellow solution. Then the ethanol solution of the citric acid, with the citric acid to titanium molar ratio (CTR) as 1:12, 1:6, and 1:4, were added to this yellow solution under constant stirring, respectively. The mixed solution was then stirred at RT for about 20 h to form a white sticky gel. After aged in air for several hours, the resulting gel was dried at 100 °C over 10 h and then ground completely. The gel precursors were calcined at 800 °C for 15 h in Ar atmosphere to obtain $Li_4Ti_5O_{12}$/C composites. $Li_4Ti_5O_{12}$/C composites prepared with citric acid to titanium molar ratio, CTR = 1:12, 1:6, and 1:4 were labeled as $Li_4Ti_5O_{12}$/C-1, $Li_4Ti_5O_{12}$/C-2 and $Li_4Ti_5O_{12}$/C-3, respectively.

2.2. Characterization of $Li_4Ti_5O_{12}$/C composites

The amount of the carbon in $Li_4Ti_5O_{12}$/C composites was measured by a thermal gravimetric (TG) method using a TG–DSC analyzer (Model NETZSCH STA449C, Germany) from RT to 850 °C at a heating rate of 10 °C min^{-1} in air. The crystal structure of the synthesized powders was examined by X-ray diffraction analysis (XRD, Model X'TRAX) using nickel filtered Cu Ka radiation (λ = 0.15406 nm) over the 2θ range from 10° to 80°. The particle morphology of the powders was observed using JEOL-6930 scanning electron microscopy (SEM) and a Joel JEM-1010 transmission electron microscopy (TEM). The properties of the porous system in the pore sizes range from 1.7 to 300 nm were determined by nitrogen adsorption at room temperature using a 3H-2000 specific surface area instrument (Beishide Instrument-ST Co., Ltd., Beijing). Before the distribution of pore size evaluation, the samples of mass around 100 mg were evacuated at 200 °C under 0.1 Pa prior the adsorption.

2.3. Electrochemical characterization $Li_4Ti_5O_{12}$/C composites

Electrochemical properties of the samples were measured with the assembling swagelok cell, for which Li metal was used as the counter and reference electrode. The electrolyte was 1 M $LiPF_6$ in ethylene carbonate and diethyl carbonate (EC-DMC 1:1, v/v). The Celgard 3501 polypropylene micro-porous film was used as the separator. The $Li_4Ti_5O_{12}$ electrode was prepared by mixing 85 wt% $Li_4Ti_5O_{12}$ active material, 10 wt% carbon black (Super P) and 5 wt% polyvynilidene fluoride (PVDF) binder dispersed in enough N-methyl-2-pyrrolidine (NMP). Then, the viscous slurry was cast on a copper foil as the current collector by a Dr. Blade. After drying overnight under vacuum at 100 °C to remove the solvent, the electrode was punched to a disk shape with a diameter of 16 mm for the half-cell test. The cell was assembled in a dry glove box filled with high purity argon gas. The galvanostatic discharge–charge tests were carried out using a BT-2000 battery testing system (Arbin, USA) in the voltage range of 1.0–3.0 V versus Li^+/Li. Electrochemical impedance spectroscopy was performed by a CHI660B electrochemical workstation (Shanghai Chenhua Instrument Co. Ltd., China) in the frequency range from 0.1 Hz to 1 MHz. Cyclic voltammograms were recorded from 1 to 3 V versus Li^+/Li at the scanning rate of 0.2 mV s^{-1} using a CHI660B electrochemical workstation.

3. Results and discussion

Fig. 1 displays the XRD patterns of the obtained $Li_4Ti_5O_{12}$/C composites prepared with different content of citric acid in the xerogel precursors. All of the observed diffraction peaks can be indexed to spinel $Li_4Ti_5O_{12}$ (JCPDS file No. 26-1198). The XRD results prove that the amount of citric acid does not influence the formation of spinel $Li_4Ti_5O_{12}$ phase. The absence of carbon in the XRD patterns is attributed to its low content or amorphous structure. In addition, with increasing the amount of the citric acid in the precursors, the diffraction peak intensity of the $Li_4Ti_5O_{12}$/C composites decreases indicating that the carbon in the composites may be in an amorphous state.

The SEM images of the obtained $Li_4Ti_5O_{12}$/C composites are presented in Fig. 2. From the figure, we can see that all the samples display non-uniform fine particles with the size within the range of 200–700 nm. Some particles are aggregated into sub-micron sized particles. In addition, the surface of the $Li_4Ti_5O_{12}$ particles is not smooth, since the fine carbon particles distribute on the surface of $Li_4Ti_5O_{12}$ particles. Guerfi et al. [14] pointed out that the carbon additive can help to reduce the particle size and produce an agglomerate of small particles in a chain-like structure. The carbon from the pyrolysis of citric acid distributes between the $Li_4Ti_5O_{12}$ particles. It can hinder the agglomerate of $Li_4Ti_5O_{12}$ particles and

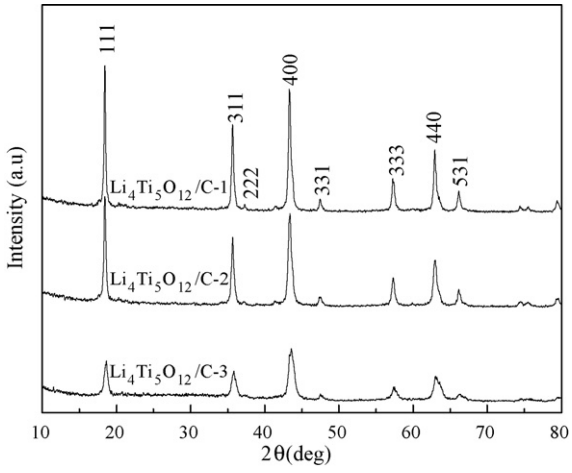

Fig. 1. XRD patterns of $Li_4Ti_5O_{12}$/C composites obtained from heating the xerogel at 800 °C for 15 h.

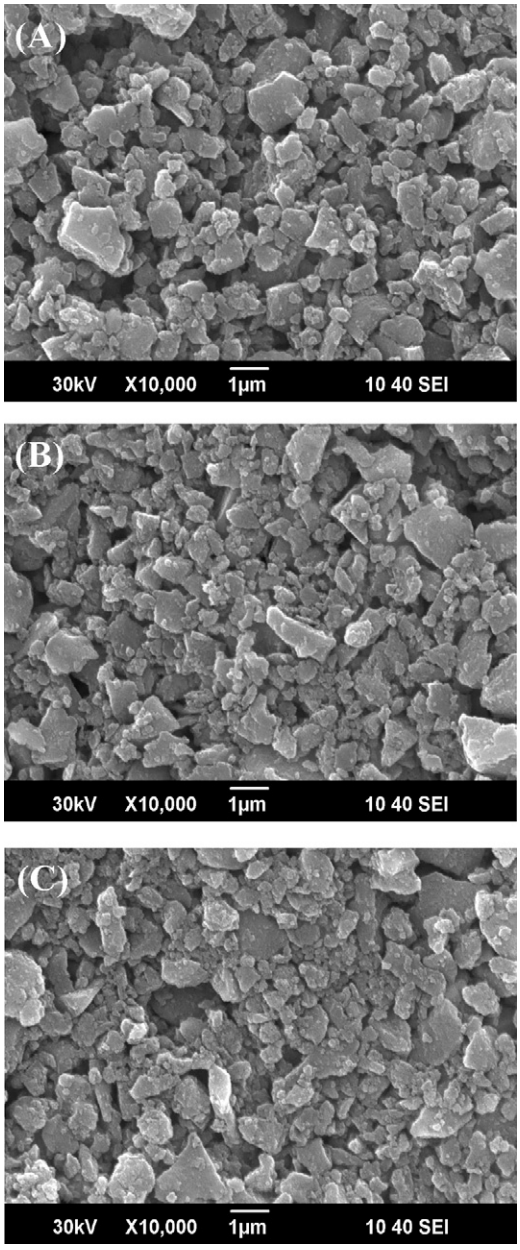

Fig. 2. SEM images of (A) $Li_4Ti_5O_{12}$/C-1, (B) $Li_4Ti_5O_{12}$/C-2 and (C) $Li_4Ti_5O_{12}$/C-3.

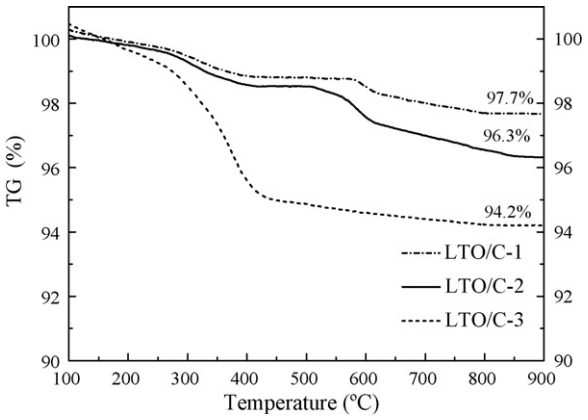

Fig. 3. TG/DSC curve of the $Li_4Ti_5O_{12}$/C composites under air atmosphere with a heating rate of 10 °C min^{-1}.

retard the growth of particles during sintering. The small particles can shorten the diffusion path for Li^+ and then improve the electrochemical properties of the composites.

The carbon contents of the $Li_4Ti_5O_{12}$/C composites were determined by the TG method. The TG curves of the $Li_4Ti_5O_{12}$/C composites performed in a flowing air atmosphere are shown in Fig. 3. The slight weight loss before 200 °C can be assigned to the removal of water. Weight loss of about 0.3%, 0.2% and 0.3% due to the removal of water can be observed on the TG curves for $Li_4Ti_5O_{12}$/C-1, $Li_4Ti_5O_{12}$/C-2 and $Li_4Ti_5O_{12}$/C-3 samples, respectively. There is no extremely distinct weight loss on the TG curves after 850 °C. Thus, the carbon contents in the $Li_4Ti_5O_{12}$/C composites are turned out to be approximately 2%, 3.5% and 5.5%, with increasing the amount of citric acid in the starting xerogel. The color of the $Li_4Ti_5O_{12}$/C composites changes from gray to black, which also proves that the carbon amount of the samples increases with increasing the amount of citric acid in the starting xerogel. The carbon in the composites is created from the pyrolysis of citric acid. If we resume the thermal decomposition of citric acid follows the reaction $C_6H_8O_7{\cdot}H_2O \rightarrow 1.5CO_2 + 5H_2O + 4.5C$ to completion, theoretical carbon contents of 4.7%, 8.9% and 12.8% would be reached for $Li_4Ti_5O_{12}$/C-1, $Li_4Ti_5O_{12}$/C-2 and $Li_4Ti_5O_{12}$/C-3 samples. However, the actual decomposition process is much more complicated. Gu et al. [29] reported that in addition to CO_2 and H_2O, CO and H_2 were also detected in the effluent gas when citric acid was calcined at 700 °C, suggesting that carbon contents of the composites could be much lower than theoretical carbon contents according to the above reaction. It is well known that one citric acid molecule has six C atoms in the structure out of those six C atoms, four of which have bonds with oxygen. Thus, it is expected that all those four C atoms will be lost during the thermal degradation of citric acid. If the decomposition of citric acid proceeds by one of following reactions:

$$C_6H_8O_7{\cdot}H_2O = 4CO_2 + 5H_2 + 2C \quad (1)$$

$$C_6H_8O_7{\cdot}H_2O = 2CO_2 + 5H_2 + 4CO + C \quad (2)$$

then the theoretical carbon contents in the $Li_4Ti_5O_{12}$/C composites can be estimated as shown in Table 1. TG analysis showed the carbon contents of the composites were about 2%, 3.5% and 5.5% for $Li_4Ti_5O_{12}$/C-1, $Li_4Ti_5O_{12}$/C-2 and $Li_4Ti_5O_{12}$/C-3 samples, respectively. The analytically obtained carbon contents are much lower than that determined according to the reactions (1), but higher than that estimated from reaction (2). Moreover, amounts of black tars can be observed in the cooling zone of the furnace tube after the decomposition of citric acid, suggesting some citric acid may decompose to lower molecular-weight volatile organics which were lost by evaporation [29]. This part of citric acid cannot contribute to the formation of solid carbon. Therefore, the real carbon contents in the composites are much smaller than expected. The degradation of citric acid depends on many parameters, such as the heating regime and the composition of the precursors, and one of the most important factors is the heating regime [30–32]. Moskon et al. [31] reported that the heating rates and the plateau value of carbonization temperature were the crucial parameters affecting the process of carbonization of citric acid. With lower heating rates, the process of carbonization becomes less vigorous, that is, it involves lower rates of gas evolution, which results in smaller losses of solid carbonized material [31]. Even more the real pyrolysis process of citric acid is much more complicated, we even resume the complicated decomposition process of citric acid mainly went towards the combination of reactions (1) and (2).

Table 1
Summaries of the estimated results of the composites carbon contents according to reactions (1) and (2).

Samples	Carbon content (%) estimated according to different reactions	
	Reaction (1)	Reaction (2)
LTO/C-1	2.13	1.08
LTO/C-2	4.17	2.13
LTO/C-3	6.13	3.16

Fig. 4 shows TEM micrographs of the $Li_4Ti_5O_{12}$/C composites. It can be seen that the $Li_4Ti_5O_{12}$ particles in all composites are coated with non-uniform carbon layers (about 2–10 nm), which are expected to reinforce the internal contact of $Li_4Ti_5O_{12}$ particles and enhance the electrical conductivity of $Li_4Ti_5O_{12}$/C composites. Furthermore, with a higher content of citric acid in the starting xerogel, a much thicker carbon coating appears. TEM micrographs indicate that the amount of citric acid in the starting xerogel plays an important role during the thermal decomposition of the xerogels.

Recently, Gaberscek et al. [33–35] reported porous, carbon-decorated $LiFePO_4$ prepared by sol–gel method based on citric acid. SEM image and TEM micrograph show that all particles seem to be porous with pore sizes ranging from micrometer to nanometer range. The presence of nanoporosity was confirmed by BET measurements (total surface area was about 60 m^2/g) and N_2 adsorption data (a large portion of pores with average diameter of about 10 nm was detected) [34]. Zhang et al. [36] also demonstrated that citric acid can be decomposed into porous carbon around 600 °C. However, in our study, SEM image and TEM micrograph show no any microscopic and sub-microscopic pores in the $Li_4Ti_5O_{12}$/C composites. To further explore the presence of nanopore in the composites, the distribution of pore sizes was determined by nitrogen adsorption in the pore sizes range from 1.7 to 300 nm. As shown in Fig. 5, significant nanoporosity with a relatively narrow distribution of pore sizes was surprisingly found in the $Li_4Ti_5O_{12}$/C composites. A large portion of pores with average diameter of about 4 nm can be detected, and the pore volume significantly increases with increasing the amount of citric acid in the starting xerogel. The present results clearly demonstrate that citric acid can be decomposed into nanoporosity carbon after sintering at 800 °C in Ar atmosphere. The total pore volume of pores with a diameter smaller than 220 nm is 0.037, 0.042 and 0.062 cm^3/g, and the total surface area was about 10.5, 18.8, 32.3 m^2/g, for the $Li_4Ti_5O_{12}$/C-1, $Li_4Ti_5O_{12}$/C-2 and $Li_4Ti_5O_{12}$/C-3 composites, respectively. Gaberscek et al. [34] reported the total pore volume of pores with a diameter smaller than 180 nm was 0.11 cm^3/g. The difference may be partly due to the route of heat treatment as well as the synthesis process. The results also demonstrate that the amount of citric acid in the starting xerogel not only determines the carbon content, but also significantly affects the distribution of pore sizes and the surface area. As observed from TEM micrographs, the relatively large differ-

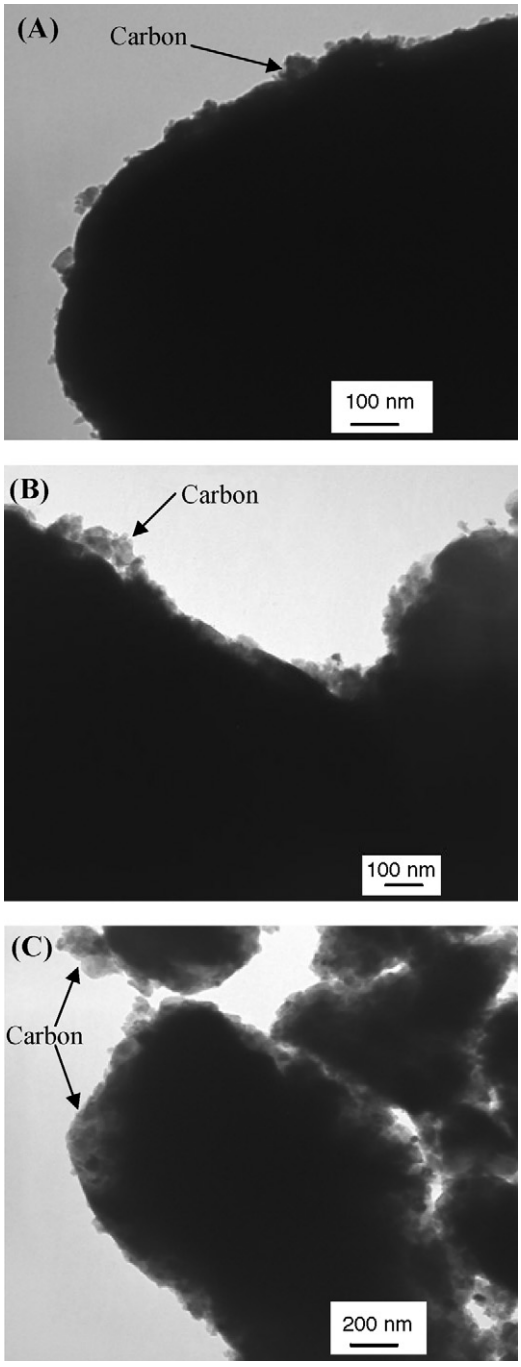

Fig. 4. TEM image of (A) $Li_4Ti_5O_{12}$/C-1, (B) $Li_4Ti_5O_{12}$/C-2 and (C) $Li_4Ti_5O_{12}$/C-3 composites.

ences of carbon coating between samples may be more or less due to porosity of carbon. From the measured carbon content and the total surface area, and assuming that carbon (density = ca 1.8 g/cm^3) covers uniformly all the materials surfaces, we can easily evaluate that the approximate carbon coating thickness should be 1.1, 1.0 and 0.9 nm, for the $Li_4Ti_5O_{12}$/C-1, $Li_4Ti_5O_{12}$/C-2 and $Li_4Ti_5O_{12}$/C-3 composites, although slightly below the range estimated from TEM micrographs (2–10 nm) as shown in Fig. 4. This may indicated that either the carbon density is lower than assumed or carbon layer is not continuous over the whole BET surface area. As shown in Fig. 4, the observed thickness is not uniform along the whole surface. Gaberscek et al. [34] pointed out that non-uniform carbon layers as a structural imperfection may in fact be desirable from

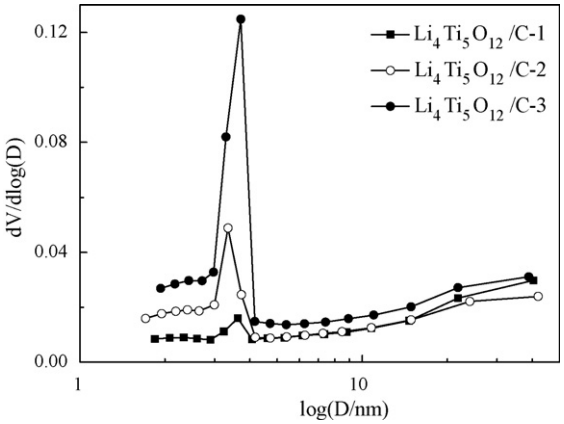

Fig. 5. BJH distribution of pore sizes from the desorption branch for the $Li_4Ti_5O_{12}$/C composites.

the electrochemical view point that the exposed surface of active material facilitates the access of Li^+ to the sites where the electrochemical reaction takes place. In conclusion, it is worth pointing out two-fold role of the in situ carbon as following: (1) it can form a large number of point contacts on the surface of each active particle and provide good inter-particle electronic conductivity and (2) it creates nanoporosity carbon in the electrode composites which are necessary for Li^+ conduction needed at high rates.

The discharge–charge curves in the first cycle of the $Li_4Ti_5O_{12}$/C composites measured at 0.1C rate between 1.0 and 3.0 V versus Li^+/Li are shown in Fig. 6. Both samples $Li_4Ti_5O_{12}$/C-1 and $Li_4Ti_5O_{12}$/C-2 exhibit extremely flat discharge/charge plateaus at the voltage about 1.5–1.6 V (versus Li^+/Li). Moreover, the small potential difference, only 60 mV, between charge and discharge plateau reflects that the polarization of both samples $Li_4Ti_5O_{12}$/C-1 and $Li_4Ti_5O_{12}$/C-2 is very low. However, the charge plateau of the sample $Li_4Ti_5O_{12}$/C-3 departs from the standard potential gradually. The main reason is perhaps due to high resistance of the electrode, which causes the high polarization of the electrode. The sample $Li_4Ti_5O_{12}$/C-2 exhibits the best electrochemical performance with a discharge specific capacity of 174 mAh g^{-1} and 88.2% coulombic efficiency, while the sample $Li_4Ti_5O_{12}$/C-3 exhibits a specific capacity of only 133.4 mAh g^{-1} in the first cycle. The lowest reversible capacities were obtained for the composites with the highest carbon content and the largest volume of pores. Therefore, it can be concluded that the excess carbon in the composites does not inevitably enhance the reversible capacity of the sample. The specific cause will be investigated subsequently.

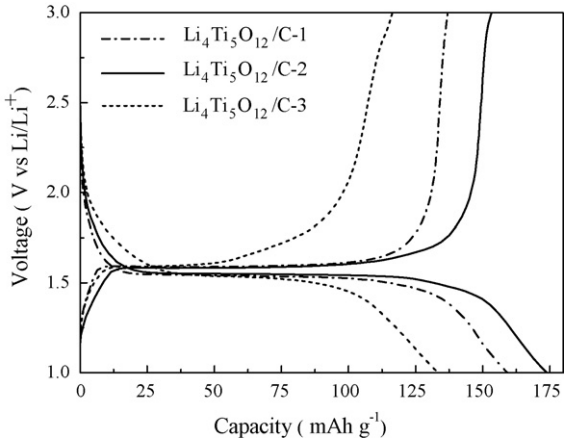

Fig. 6. Discharge–charge curves at 0.1C of $Li_4Ti_5O_{12}$/C composites.

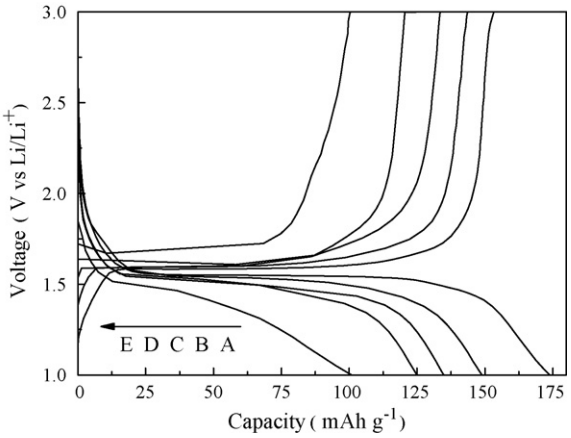

Fig. 7. Discharge–charge curves in the first cycle at different C-rates of $Li_4Ti_5O_{12}$/C-2: (A) 0.1C, (B) 0.5C, (C) 1C, (D) 2C and (E) 5C.

The discharge–charge curves of the sample $Li_4Ti_5O_{12}$/C-2 at different C-rates from 0.1C to 5C are shown in Fig. 7. The delithiation capacities are 153.3, 143.6, 133.5, 124.7 and 100.5 mAh g^{-1}, at 0.1C, 0.5C, 1C, 2C and 5C, respectively. The difference between charge and discharge plateau is only 60 mV even the current is as high as 2C, indicating the low polarization of $Li_4Ti_5O_{12}$/C electrodes with 3.5 wt% carbon coating. The discharge plateau potentials at 0.1C and 0.5C are very close to the reversible redox potential of spinel $Li_4Ti_5O_{12}$ (1.55 V), as reported by Scharner et al. [37], but decrease gradually from 1.55 V at 0.1C to 1.48 V at 5C, which can be ascribed to the polarization of the electrode at high current.

Long term cycling behaviors of the sample $Li_4Ti_5O_{12}$/C-2 at different C-rates from 0.1C to 5C are also investigated in this paper and the results are shown in Fig. 8. The delithiation capacities after 50 charge–discharge cycles are 140.4, 129.2, 118.1, 109.7 and 86.1 mAh g^{-1} at 0.1C, 0.5C, 1C, 2C and 5C, respectively. The corresponding capacity fading rates at these C-rates are calculated to be 0.17%, 0.2%, 0.23%, 0.24% and 0.29% per cycle, respectively. The excellent cycling stability can be attributed to the good crystallinity of this sample and the improvement of the electrical conductivity via carbon coating.

To further demonstrate the effect of carbon content and the pore volume on the electrochemical performance of the electrode, the A.C. impedance of $Li_4Ti_5O_{12}$/C composites at the state of discharging (40% DOD) was measured. The impedance spectra were recorded after two formation cycles. As shown in Fig. 9, the impedance curves of all three samples are comprised a depressed semicircle in high to medium frequency range and a spike in the low frequency range. It is well known that the cross-section value of impedance spectra on the real Z' axis at the high frequency is the internal resistance, R_i, corresponding the resistance of electrolyte mainly, while the semicircle is corresponding to the electrochemical reaction resistance and the double layer capacity of the electrode. The inclined line in the lower frequency range is attributed to the Warburg impedance, which is associated with solid-state diffusion of Li^+ through the bulk of $Li_4Ti_5O_{12}$. As shown in Fig. 9, the $Li_4Ti_5O_{12}$/C-2 sample exhibits the lowest electrochemical reaction resistance, which is consistent with the result of the best reversible capacities. The difference in the resistance can be ascribed to the difference in the transport path of electrons and Li^+ between three electrodes. For the $Li_4Ti_5O_{12}$/C composites with high carbon content, numerous electronic conductive phase forms the coating around most active particle; thus, most spots on the particle surface can accept the electrons. Such carbon coating can improve the electrochemical performance of the composites by the improved electrical wiring of the $Li_4Ti_5O_{12}$ particles. However, the excessive carbon layer in the composites does not improve significantly the electronic conductivity of the composites. Rather than that, it introduces additional holdbacks for Li^+ and electrolyte penetration. The phenomena can be explained by assuming that superfluous carbon coatings are less permeable for Li^+ due to non-perfect electrochemical wiring. As reported by Dominko et al. [33] the excess carbon may introduce an additional barrier for Li^+ and electrolyte penetration. Gaberscek and Jamnik [38] also found that any increase of coating thickness in the studied range resulted in a decrease of the electrode performance. Thus, the carbon content should be appropriate to ensure that the carbon layer must be permeable for the accessibility of Li^+. On the other hand, the nanoporosity carbon in the composites is necessary for the transport of Li^+. Due to the porosity of the electrode, the liquid electrolyte can effectively soak all particles and penetrate easily through the carbon coatings due to electrode porosity, thus ensuring the active particles with a maximum concentration of Li^+. In addition, the pores connecting with each other can easily bring into electrical contact. Thus, a high pore volume can effectively reduce the ionic conductivity of the $Li_4Ti_5O_{12}$ composites. As the results of the BET measurements, the pore volume significantly increases with increasing the carbon content of $Li_4Ti_5O_{12}$/C composites. However, the excessive carbon in the composites introduces additional holdbacks for the transport of Li^+. Thus, it is very difficult to distinguish and evaluate the carbon content on the ionic conductivity of the $Li_4Ti_5O_{12}$/C composites. Actually, for general mixed ionic and electronic conductor, the total impedances are affected by the ionic

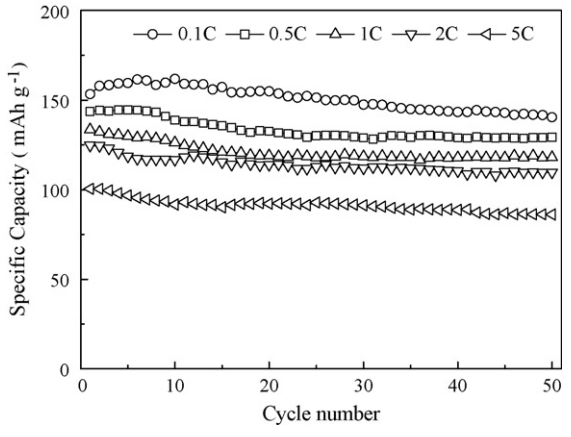

Fig. 8. Cycling performance (delithiation capacities) at different C-rates of $Li_4Ti_5O_{12}$/C-2.

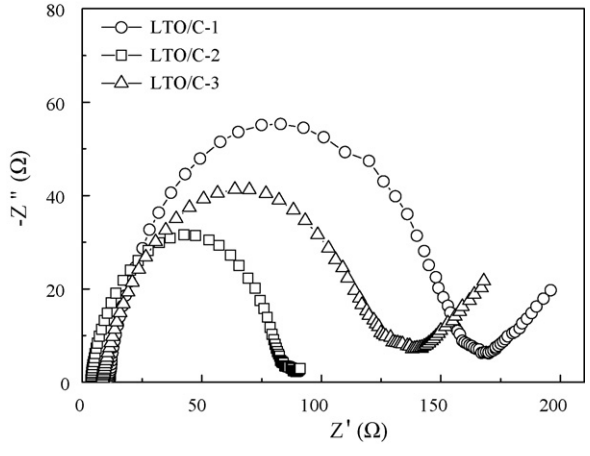

Fig. 9. Impedance spectra of (A) $Li_4Ti_5O_{12}$/C-1, (B) $Li_4Ti_5O_{12}$/C-2 and (C) $Li_4Ti_5O_{12}$/C-3 at the state of discharging (40% DOD).

and electronic resistivity. The total electrical conductivity can be described by

$$\sigma_t = \sigma_i + \sigma_e \quad (3)$$

where σ_t is the total conductivity, σ_i is the ionic conductivity and σ_e is the electronic conductivity.

As the active material of lithium-ion batteries, $Li_4Ti_5O_{12}$ is a mixed conductor. The charge/discharge process in the electrode of lithium-ion batteries, however, is not a simple electrical conducting process but a complex reaction process. The ionic and electronic conduction are not two independent processes. They are limited and influenced by each other. For the $Li_4Ti_5O_{12}$/C composites, the electronic conductivity will increase with increasing the amount of citric acid in the starting xerogel due to a large number of point contacts for electrons to the surface of the active material, whereas the excessive carbon in the composites may reduce the Li^+ conductivity owing to the additional holdbacks for the transport of Li^+. In summary, the carbon content of the $Li_4Ti_5O_{12}$/C composites should be optimized to supply the sufficient electronic and ionic conductivity for improving the electrochemical performance of the electrodes. The carbon content in the $Li_4Ti_5O_{12}$/C composites with best electrochemical performance is about 3.5 wt% in our study. The results agree well with that of the discharge–charge measurements.

Fig. 10 shows cyclic voltammograms of the sample $Li_4Ti_5O_{12}$/C-2 at a scan rate of 0.2 mV s^{-1} between 3.0 and 1.0 V versus Li^+/Li. The cathodic peak shows larger area compared with the anodic peak during the first cycle, which can be attributed to the irreversible capacity. From the second cycle, the cyclic voltagemmetric curves coincide with each other; meanwhile, the ratio of I_{pa}/I_{pc} nearly equals to 1, therefore the kinetics of lithium intercalation and deintercalation is reversible. For a reversible reaction, the diffusion coefficient can be calculated by the following equation [39,40]:

$$I_p = 2.69 \times 10^5 A n^{2/3} C_0 D^{1/2} \nu^{1/2} \quad (\text{at } 25\,^\circ\text{C}) \quad (4)$$

where I_p is the peak current of the reduction peak, A is the electrode area in cm^2, n is the number of electrons per molecule during the intercalation, C_0 is the concentration of Li^+ in mol cm^3, D is the diffusion coefficient of Li^+ and ν is scan rate in V s^{-1}. According to the Eq. (4), the calculated D_{Li^+} in the electrode is 1.68×10^{-10} cm^2 s^{-1}, which is at the range of 2×10^{-8} to 2×10^{-12} cm^2 s^{-1} and consistent with the results reported by Rho and Kanamura [41]. As above mentioned, the citric acid sol–gel method is a promising technique to prepare $Li_4Ti_5O_{12}$/C composites with an excellent electrochemical performance.

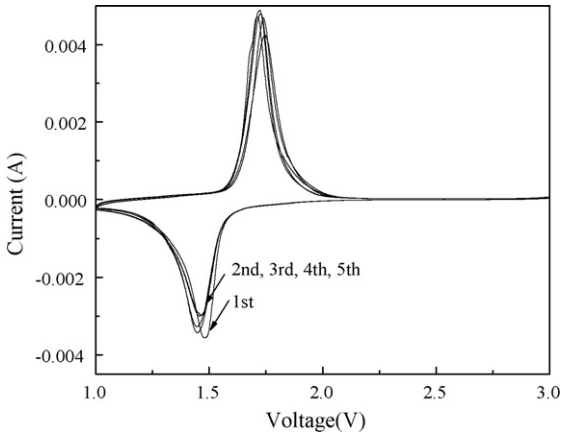

Fig. 10. Cyclic voltammograms of the sample $Li_4Ti_5O_{12}$/C-2 at a scanning rate of 0.2 mV s^{-1}.

4. Conclusions

Well crystallized $Li_4Ti_5O_{12}$/C composites with different carbon content have been prepared by a sol–gel method with citric acid as the chelating agent and carbon resource. The initial amount of the carbon source in the starting xerogel is a critical factor which determines the content of the coated carbon and the pore volume, therefore governs the high rate performance of the $Li_4Ti_5O_{12}$. Even though low carbon content in $Li_4Ti_5O_{12}$/C composites cannot provide the sufficient electronic conductivity, the excess carbon may come into being holdbacks and hinder the mobility of lithium ions. The best-performing as-prepared $Li_4Ti_5O_{12}$/C composites, with sub-micron size and in situ surface carbon coating of 3.5 wt%, delivered delithiation capacities of 143.6 and 133.5 mAh g^{-1} at 0.5C and 1C rates, respectively, without obvious capacity fade up to 50 cycles. The results show that the citric acid sol–gel method is a promising technique to prepare $Li_4Ti_5O_{12}$/C composites with an excellent electrochemical performance.

Acknowledgements

This work is financially supported by the National Basic Research Program of China (973 Program) (the Project No. 2007CB2097050) and the National Science Foundation of China (the Project No. 20803035). J.W. also acknowledges the financial support from the Minhang Science and Technology Program of Shanghai (the Project No. 2009MH188).

References

[1] H. Yang, H. Bang, K. Amine, J. Prakash, J. Electrochem. Soc. 152 (2005) A73.
[2] H. Yang, S. Amiruddin, H. Bang, Y.K. Sun, J. Prakash, J. Ind. Eng. Chem. 12 (2006) 12.
[3] H. Yang, X.D. Shen, J. Power Sources 167 (2007) 515.
[4] T. Ohzuku, A. Ueda, N. Yamamoto, J. Electrochem. Soc. 142 (1995) 1431.
[5] K. Mukai, K. Ariyoshi, T. Ohzuku, J. Power Sources 146 (2005) 213.
[6] K. Zaghib, M. Simoneau, M. Armand, M. Gauthier, J. Power Sources 81–82 (1999) 300.
[7] C.H. Chen, J.T. Vaughey, A.N. Jansen, D.W. Dees, A.J. Kahaian, T. Goacher, M.M. Thackeray, J. Electrochem. Soc. 148 (2001) A102.
[8] T. Yuan, K. Wang, R. Cai, R. Ran, Z.P. Shao, J. Alloys Compd. 477 (2009) 665.
[9] M.W. Raja, S. Mahanty, M. Kundu, R.N. Basu, J. Alloys Compd. 468 (2009) 258.
[10] G.F. Yan, H.S. Fang, H.J. Zhao, G.S. Li, Y. Yang, L.P. Li, J. Alloys Compd. 470 (2009) 544.
[11] T. Yuan, R. Cai, R. Ran, Y.K. Zhou, Z.P. Shao, J. Alloys Compd. (2010), doi:10.1016/j.jallcom.2010.04.253.
[12] K. Nakahara, R. Nakajima, T. Matsushima, H. Majima, J. Power Sources 117 (2003) 131.
[13] L.X. Yang, L.J. Gao, J. Alloys Compd. 485 (2009) 93.
[14] A. Guerfi, S. Sévigny, M. Lagacé, P. Hovington, K. Kinoshita, K. Zaghib, J. Power Sources 88 (2003) 119–121.
[15] X. Li, M.Z. Qu, Z.L. Yu, J. Alloys Compd. 487 (2009) L12.
[16] S.H. Huang, Z.Y. Wen, X.J. Zhu, Z.X. Lin, J. Electrochem. Soc. 152 (2005) A186.
[17] T.F. Yi, J. Shu, Y.R. Zhu, X.D. Zhu, R.S. Zhu, A.N. Zhou, J. Power Sources 195 (2010) 285.
[18] H.L. Zhao, Y. Li, Z.M. Zhu, J. Lin, Z.H. Tian, R.L. Wang, Electrochim. Acta 53 (2008) 7079.
[19] S.H. Huang, Z.Y. Wen, X.J. Zhu, Z.H. Gu, Electrochem. Commun. 6 (2004) 1093.
[20] S.H. Huang, Z.Y. Wen, X.J. Zhu, Z.X. Lin, J. Power Sources 165 (2007) 408.
[21] S.H. Huang, Z.Y. Wen, J.C. Zhang, X.L. Yang, Electrochim. Acta 52 (2007) 3704.
[22] S.H. Huang, Z.Y. Wen, X.J. Zhu, X.L. Yang, J. Electrochem. Soc. 152 (2005) A1301.
[23] J.J. Huang, Z.Y. Jiang, Electrochim. Acta 53 (2008) 7756.
[24] G.J. Wang, J. Gao, L.J. Fu, N.H. Zhao, Y.P. Wu, T. Takamura, J. Power Sources 174 (2007) 1109.
[25] L. Cheng, X.L. Li, H.J. Liu, H.M. Xiong, P.W. Zhang, Y.Y. Xia, J. Electrochem. Soc. 154 (2007) A692.
[26] J. Gao, J.R. Ying, C.Y. Jiang, C.R. Wan, J. Power Sources 166 (2007) 255.
[27] L.J. Fu, H. Liu, C. Li, Y.P. Wu, E. Rahm, R. Holze, H.Q. Wu, Prog. Mater. Sci. 50 (2005) 881.
[28] J.S. Yang, J.J. Xu, J. Electrochem. Soc. 153 (2006) A716.
[29] P. Gu, R. Cai, Y.K. Zhou, Z.P. Shao, Electrochim. Acta 55 (2010) 3876.
[30] R. Dominko, J.M. Goupil, M. Bele, M. Gaberscek, M. Remskar, D. Hanzel, J. Jamnik, J. Electrochem. Soc. 152 (2005) A858.
[31] J. Moskon, R. Dominko, M. Gaberscek, R. Cerc-Korosec, J. Jamnik, J. Electrochem. Soc. 153 (2006) A1805.
[32] R. Dominko, M. Bele, M. Gaberscek, A. Meden, M. Remskar, J. Jamnik, Electrochem. Commun. 8 (2006) 217.

[33] R. Dominko, M. Bele, M. Gaberscek, M. Remskar, D. Hanzel, S. Pejovnik, J. Jamnik, J. Electrochem. Soc. 152 (2005) A607.
[34] M. Gaberscek, R. Dominko, M. Bele, M. Remskar, D. Hanzel, J. Jamnik, Solid State Ionics 176 (2005) 1801.
[35] R. Dominko, M. Bele, J.M. Goupil, M. Gaberscek, D. Hanzel, I. Arcon, J. Jamnik, Chem. Mater. 19 (2007) 2960.
[36] D. Zhang, X. Yu, Y. Wang, R. Cai, Z.P. Shao, X.Z. Liao, Z.F. Ma, J. Electrochem. Soc. 156 (2009) A802.
[37] S. Scharner, W. Weppner, P. Schmid-Beurmann, J. Electrochem. Soc. 146 (1999) 857.
[38] M. Gaberscek, J. Jamnik, Solid State Ionics 177 (2006) 2647.
[39] D.Y.W. Denis, C. Fietzek, W. Weydanz, K. Donoue, T. Inoue, H. Kurokawa, S. Fujitani, J. Electrochem. Soc. 154 (2007) A253.
[40] A.J. Bard, L.R. Faulkner, Electrochemical Methods, 2nd ed., Wiley, 2001, p. 231.
[41] Y.H. Rho, K. Kanamura, J. Solid State Chem. 177 (2004) 2094–2100.